Trichoplein and Aurora A block aberrant primary cilia assembly in proliferating cells

Akihito Inoko,[1] Makoto Matsuyama,[1] Hidemasa Goto,[1,2] Yuki Ohmuro-Matsuyama,[1] Yuko Hayashi,[1] Masato Enomoto,[1,2] Miho Ibi,[1] Takeshi Urano,[3] Shigenobu Yonemura,[4] Tohru Kiyono,[5] Ichiro Izawa,[1] and Masaki Inagaki[1,2]

[1]Division of Biochemistry, Aichi Cancer Center Research Institute, Chikusa-ku, Nagoya 464-8681, Japan
[2]Department of Cellular Oncology, Graduate School of Medicine, Nagoya University, Showa-ku, Nagoya 466-8550, Japan
[3]Department of Biochemistry, Shimane University School of Medicine, Izumo 693-8501, Japan
[4]RIKEN Center for Developmental Biology, Chuo-ku, Kobe 650-0047, Japan
[5]Division of Virology, National Cancer Center Research Institute, Chuo-ku, Tokyo 104-0045, Japan

The primary cilium is an antenna-like organelle that modulates differentiation, sensory functions, and signal transduction. After cilia are disassembled at the G0/G1 transition, formation of cilia is strictly inhibited in proliferating cells. However, the mechanisms of this inhibition are unknown. In this paper, we show that trichoplein disappeared from the basal body in quiescent cells, whereas it localized to mother and daughter centrioles in proliferating cells. Exogenous expression of trichoplein inhibited primary cilia assembly in serum-starved cells, whereas ribonucleic acid interference–mediated depletion induced primary cilia assembly upon cultivation with serum. Trichoplein controlled Aurora A (AurA) activation at the centrioles predominantly in G1 phase. In vitro analyses confirmed that trichoplein bound and activated AurA directly. Using trichoplein mutants, we demonstrate that the suppression of primary cilia assembly by trichoplein required its ability not only to localize to centrioles but also to bind and activate AurA. Trichoplein or AurA knockdown also induced G0/G1 arrest, but this phenotype was reversed when cilia formation was prevented by simultaneous knockdown of IFT-20. These data suggest that the trichoplein–AurA pathway is required for G1 progression through a key role in the continuous suppression of primary cilia assembly.

Introduction

The centrosome is composed of two orthogonally arranged centrioles surrounded by pericentriolar material. It functions as the primary microtubule (MT)-organizing center in animal cells. In addition, the older (or mother) centriole plays a crucial role in ciliogenesis. In most nondividing cells, the centrosome moves to the cell surface where the mother centriole is converted to a basal body, which then nucleates a cilium. Thus, so-called primary cilia are found as nonmotile projections in most types of quiescent vertebrate cells. They are involved in differentiation, sensory functions, and signal transduction, including Hedgehog, Wnt, and PDGF pathways (Eggenschwiler and Anderson, 2007; Berbari et al., 2009). The assembly and maintenance of primary cilia depends on several different proteins. These are classified into intraflagellar transport proteins (such as kinesin-2, cytoplasmic dynein 2, and the intraflagellar transport complex), membrane vesicle trafficking proteins (such as a small GTPase Rab8, its specific GTP exchange factor Rabin, and a complex of proteins encoded by genes mutated in Bardet–Biedl syndrome), centriolar proteins (such as Odf2, Cep164, and Ofd1), proteins implicated in the ciliopathy Meckel–Gruber syndrome (such as MKS1 and MKS3), and a secreted phospholipase PLA2G3 (Singla and Reiter, 2006; Bettencourt-Dias and Glover, 2007; Satir and Christensen, 2007; Anderson et al., 2008; Bornens, 2008; Gerdes et al., 2009; Nigg and Raff, 2009; Ishikawa and Marshall, 2011; Kobayashi and Dynlacht, 2011).

A. Inoko and M. Matsuyama contributed equally to this paper.

Correspondence to Masaki Inagaki: minagaki@aichi-cc.jp

Y. Ohmuro-Matsuyama's present address is Dept. of Chemistry and Biotechnology and Dept. of Bioengineering, Graduate School of Engineering, The University of Tokyo, Bunkyo-ku, Tokyo 113-8656, Japan.

Abbreviations used in this paper: AurA, Aurora A; Dox, doxycycline; FL, full length; GAPDH, glyceraldehyde 3-phosphate dehydrogenase; HDAC-6, histone deacetylase-6; IF, intermediate filament; MBP, maltose-binding protein; MT, microtubule; Pifo, Pitchfork.

The Rockefeller University Press $30.00
J. Cell Biol. Vol. 197 No. 3 391–405
www.jcb.org/cgi/doi/10.1083/jcb.201106101

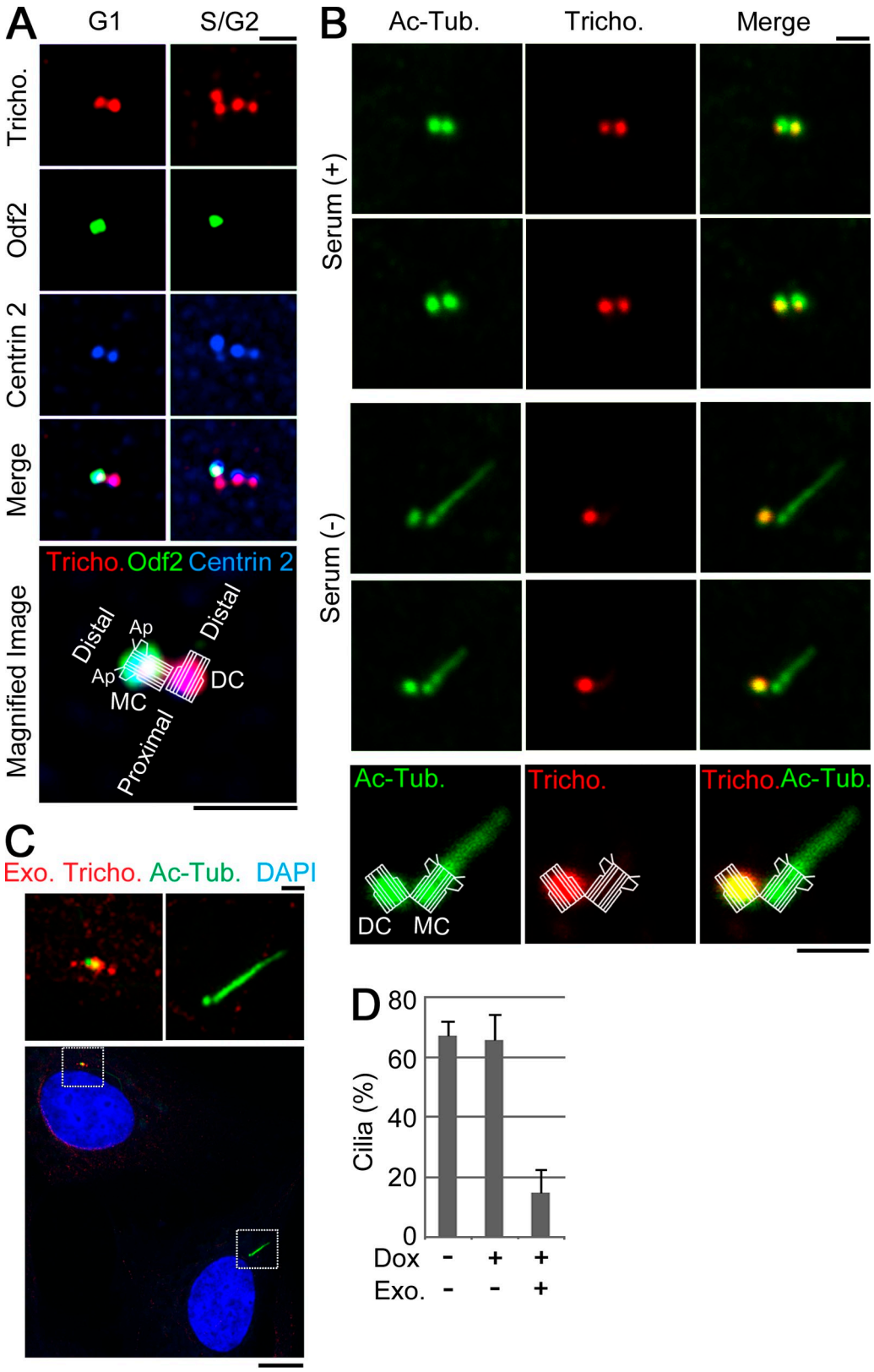

Figure 1. **Trichoplein disappears from the basal body in quiescent cells.** (A) RPE1 cells were stained with antitrichoplein (Tricho.), anti-Odf2, and anti–Centrin 2. Bottom micrograph is shown with an illustration, which indicates the structure of a mother or daughter centriole (MC or DC) with the appendage (Ap) and orientations. (B) RPE1 cells were incubated in a medium with (+) or without (−) serum and then subjected to immunofluorescence with antibodies against acetylated tubulin (Ac-Tub.) and trichoplein. (C and D) Proliferating Tet-ON RPE1 cells expressing MBP-trichoplein-Flag (Tet-FL) were incubated in a new growing medium containing 30 ng/ml doxycycline (Dox) for 4 h and then cultured in a new serum-free medium containing 30 ng/ml Dox for an additional 44 h. (C) Cells were subjected to immunostaining with anti-MBP (Exo. tricho.) and anti–acetylated tubulin or immunoblotting (Fig. 7 E). (top) Magnified insets are shown. (D) The quantification of ciliation was shown in the graph. Exo. shows the centrioles with (+) or without (−) detectable exogenous trichoplein. We analyzed 100 cells per group and calculated the percentage of ciliated cells (n = 3). Data are means ± SD. Bars: (A–C, top) 1 µm; (C, bottom) 10 µm.

Importantly, vertebrate primary cilia are resorbed upon cell cycle reentry. This resorption is considered to allow centrosomes to participate in the establishment of mitotic spindle poles, thus ensuring accurate segregation of chromosomes during cell division (Rieder et al., 1979; Tucker et al., 1979; Ehler et al., 1995; Wheatley et al., 1996; Quarmby and Parker, 2005). In contrast to molecular mechanisms underlying the assembly of cilia (and flagella), less is known about how these structures are disassembled in proliferating cells (Quarmby and Parker, 2005). Recent studies, however, attribute a key role in this process to Aurora A (AurA; Pan et al., 2004; Pugacheva et al., 2007; Kinzel et al., 2010), one of the mitotic kinases (Nigg, 2001; Carmena et al., 2009). AurA associates with HEF1 (Pugacheva et al., 2007) and Pitchfork (Pifo; Kinzel et al., 2010), and its elevated catalytic activity was reported to induce histone deacetylase-6 (HDAC-6) phosphorylation, thus stimulating HDAC-6–dependent tubulin deacetylation and destabilization of the ciliary axoneme in vertebrate cells (Pugacheva et al., 2007). Because HEF1 appears to be transiently expressed at the G0/G1 and G2/M transitions (Pugacheva et al., 2007), it is considered to mainly regulate primary cilia resorption at the G0/G1 transition. With regard to the destabilization of ciliary axoneme, Pifo was considered to have a function similar to HEF1 (Kinzel et al., 2010). Thus, both these studies emphasize a mechanism that promotes ciliary disassembly at the G0/G1 transition. How ciliary reassembly remains suppressed at subsequent cell cycle phases in proliferating cells is largely unknown.

We recently found that trichoplein, originally identified as a keratin intermediate filament (IF) scaffold protein (Nishizawa et al., 2005), was also concentrated at the subdistal/medial zone of both mother and daughter centrioles in proliferating cells (Ibi et al., 2011). Here, we show that trichoplein negatively regulates primary cilia assembly in G1 phase, which allows cell cycle progression. This trichoplein activity requires AurA binding and activation at centrioles.

Results

Trichoplein suppresses primary cilia assembly

To examine the localization of trichoplein at different cell cycle phases, we stained RPE1 (human telomerase reverse transcriptase–immortalized retinal pigment epithelia) cells with antitrichoplein antibodies. As shown in Fig. 1 A, the number of antitrichoplein signals at the centrosome exactly coincided with the number of anticentrin 2–positive spots, which corresponds to the number of centrioles (Paoletti et al., 1996; Laoukili et al., 2000). However, in serum-starved cells, antitrichoplein signals were much weaker at the basal body than at the daughter centriole, and the ciliary axoneme (visualized with anti–acetylated tubulin) was virtually unstained (Fig. 1 B). Trichoplein is therefore an authentic centriolar protein throughout the centrosome duplication cycle but notably absent from the basal body.

These observations raised the question as to whether trichoplein negatively regulates primary cilia formation. First, we analyzed the effect of exogenous trichoplein expression on primary cilia assembly in serum-starved RPE1 cells (Fig. 1, C and D). For this purpose, we established a Tet-ON RPE1 cell line allowing the expression of maltose-binding protein (MBP)– and Flag-tagged full-length trichoplein (MBP-trichoplein-Flag) in a doxycycline (Dox)-dependent manner (Tet-full length [FL]; for characterization see immunoblotting data in Fig. 7 E; Ibi et al., 2011). After induction of MBP-trichoplein-Flag expression, primary cilia formation was inhibited whenever basal bodies showed detectable anti-MBP staining but not in those few cells in which the protein was not expressed (Fig. 1, C and D, Exo. Tricho and Exo.). Thus, expression of exogenous trichoplein can suppress primary cilia formation.

Next, we analyzed the effect of trichoplein depletion from proliferating RPE1 cells (also see Materials and methods; Fig. 2). 48–72 h after transfection, a primary cilium-like structure was observed in 40–70% of the cells treated with trichoplein-specific siRNA, whereas <5% of control cells showed such structures (Fig. 2, A and B). To distinguish between primary cilia and elongated centrioles (Keller et al., 2009; Schmidt et al., 2009; Tang et al., 2009), we performed transmission electron microscopy (Fig. 2 C) and immunocytochemistry (Fig. 2 D). As shown in Fig. 2 C, the structures seen by electron microscopy in trichoplein-depleted cells resembled genuine primary cilia, characterized by the presence of membranous sheaths surrounding the axonemal MTs and a clear structural transition between the basal body and the cilium. Furthermore, the intraflagellar transport protein Polaris/IFT-88 (Pazour et al., 2000) was associated with both basal bodies and ciliary axonemes (Fig. 2 D), confirming that treatment with trichoplein-specific siRNA induced genuine primary cilia rather than elongated centrioles (Schmidt et al., 2009). This phenotype could be rescued by expressing RNAi-resistant exogenous trichoplein (Fig. 2, E–G, exo. and Exo. Tricho.), indicating that it is specific for trichoplein depletion. These results suggest that trichoplein suppresses primary cilia formation under conditions of cell proliferation.

AurA acts as an effector of trichoplein to inhibit primary cilia formation

Based on the importance of AurA in ciliary disassembly (Pan et al., 2004; Pugacheva et al., 2007; Kinzel et al., 2010), we examined AurA colocalization with trichoplein. We focused on the cell stage before centrosome duplication, when only two trichoplein signals could be detected (Fig. 1 A and Fig. 3 A). To ascertain where AurA localizes within these centrosomes, we examined two markers, Odf2 and C-Nap1, which associate with the distal/subdistal end of the mother centriole (Ishikawa et al., 2005) and the proximal ends of centrioles (Fry et al., 1998; Mayor et al., 2000), respectively. As shown in Fig. 3 A, AurA was proximal to the Odf2-stained area on the mother centriole and distal to the C-Nap1–stained area on both centrioles. Importantly, the signal of AurA overlapped with that of trichoplein on both mother and daughter centrioles (Fig. 3, A and B; and Fig. S1 A). AurA autophosphorylated at Thr288 (pAurA), indicative of activated AurA (Walter et al., 2000), was also observed at and near the areas where trichoplein and bulk AurA were colocalized (Fig. 3 B and Fig. S1 A, G1). Thus, before the onset of centrosome duplication, in G1 phase, the localization of AurA and pAurA highly correlates with that of trichoplein.

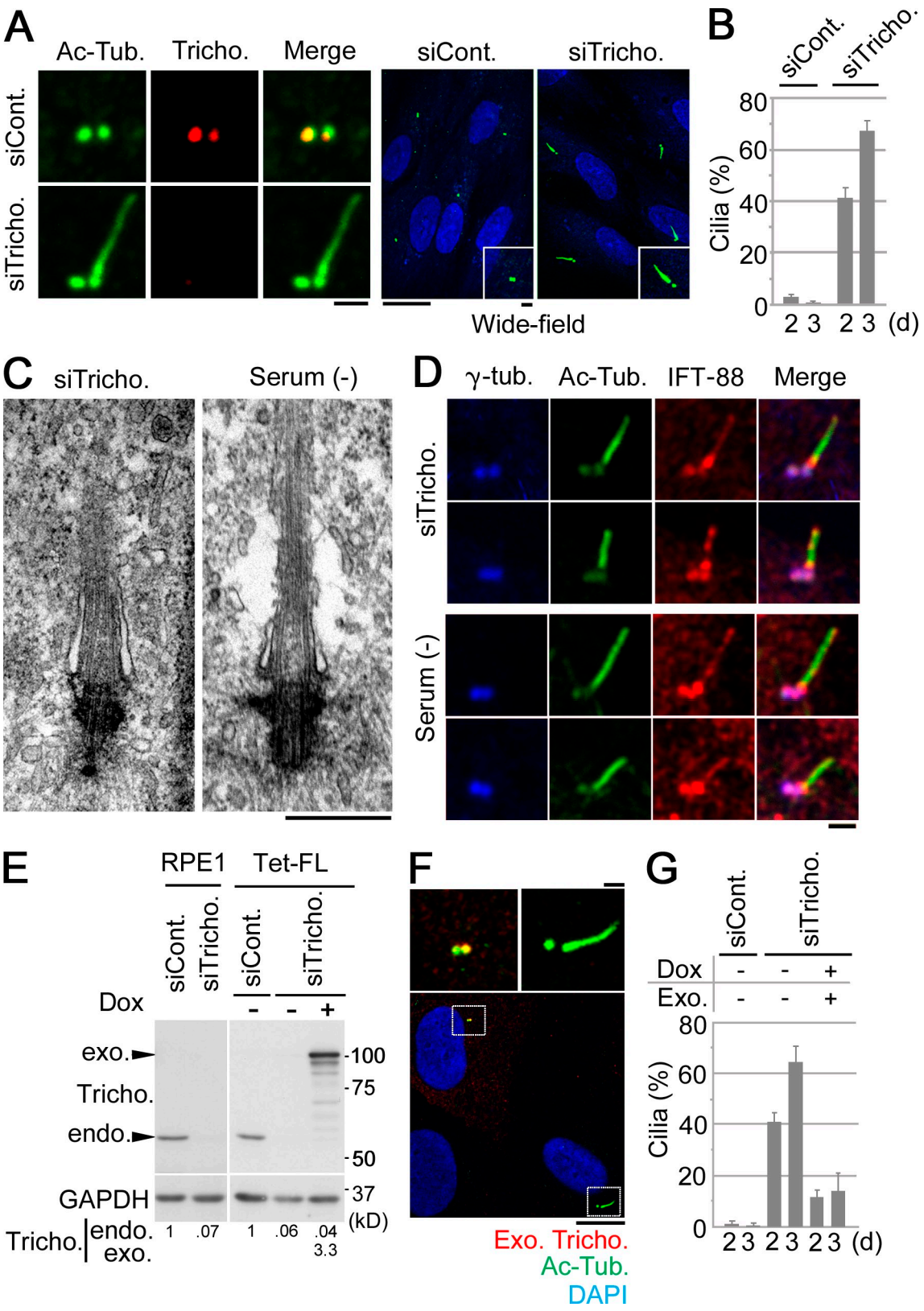

Figure 2. **Trichoplein suppresses primary cilia assembly in proliferating RPE1 cells.** (A–D) Proliferating RPE1 cells were treated with trichoplein-specific siRNA (siTricho.; targeting the 3′ untranslated region of human trichoplein mRNA) or control siRNA (siCont.) for 48 or 72 h and subjected to immunofluorescence (A). (A) Left and right images show staining with antitrichoplein (red) or DAPI (blue) in addition to anti–acetylated tubulin (Ac-Tub.; green). Insets show higher magnifications. (B) To quantify data shown in A, we analyzed 100 cells per group and calculated the percentages of cells with primary cilia-like structures 2 or 3 d after transfection ($n = 3$). (C and D) The centriolar protrusion in trichoplein-depleted cells was compared with a primary cilium formed in quiescent RPE1 cells by transmission electron microscopy (C) and immunofluorescence staining with the indicated antibodies (D). (E–G) Proliferating Tet-ON RPE1 cells expressing MBP-trichoplein-Flag (Tet-FL) and parent RPE1 cells were transfected with the indicated siRNA. 4 h after transfection

On the other hand, this correlation is no longer prominent at the G2/M transition when, as reported previously (Roghi et al., 1998), AurA and pAurA are widely distributed throughout the centrosomes, including the pericentriolar material (Fig. 3 B and Fig. S1, A and B, G2/M).

The aforementioned correlation between trichoplein and AurA localization in G1 phase led us to examine the relationship between the two proteins. We discovered that trichoplein knockdown reduced the total amount of AurA and pAurA in cells (Fig. 3 E, left; and Fig. S1 C). Moreover, AurA was less often observed at the two centrioles in cells treated with trichoplein-specific siRNA than in control siRNA-treated cells (Fig. 3 C and Fig. S1 D, quantification), and pAurA was almost completely removed from centrioles in trichoplein-depleted cells (Fig. 3 D). The observed reduction in AurA and pAurA levels as well the loss of these proteins from centrioles could be rescued by the expression of RNAi-resistant trichoplein, indicating that these phenotypes are specific to trichoplein depletion (Fig. 3, E–G; and Fig. S1, E and F, quantification). We next tested whether AurA, like trichoplein, is required for the suppression of primary cilia assembly in proliferating cells. We found that AurA depletion also induced primary cilia assembly (Fig. 4, A–D), like trichoplein depletion (Fig. 2).

Because trichoplein knockdown caused a reduction in AurA (Fig. 3 E, left; and Fig. S1 C), and knockdown of both proteins produced the same stimulatory effect on ciliation in proliferating RPE1 cells (Fig. 2 and Fig. 4, A–D), we examined whether the phenotype of trichoplein knockdown resulted from the trichoplein depletion-induced decrease of AurA expression or activity. For this, we established Tet-ON RPE1 cells expressing Myc-AurA (Tet-AurA) and checked whether AurA overexpression could rescue the phenotype of trichoplein knockdown (Fig. 4, E–I). Because the effect of AurA overexpression on cell proliferation was reported to differ among different cell types (Wang et al., 2006; Jantscher et al., 2011), we first verified that overexpression of AurA alone had little impact on cell proliferation in the case of RPE1 cells (Fig. 4, E and F). Yet, under these conditions, overexpression of exogenous AurA did not suppress the primary cilia formation that was induced by trichoplein depletion (Fig. 4, G–I, Exo. AurA and Exo.). These results rule out the possibility that the effect of trichoplein knockdown is merely caused by reduction of AurA. Instead, they suggest that AurA requires trichoplein for its ability to interfere with cilia formation. On the other hand, the AurA knockdown cells showed no reduction in trichoplein expression (Fig. S4 C, right). Thus, the presence of trichoplein alone is also insufficient to block ciliation in the absence of AurA in proliferating cells, suggesting that both AurA and trichoplein are necessary to block ciliation. Collectively, these results raise the possibility that, in proliferating cells, trichoplein inhibits ciliary reproduction through the activation of AurA.

Primary cilia–mediated effect of trichoplein depletion on cell cycle progression

Next, we examined the effect of trichoplein depletion on cell cycle progression of RPE1 cells (Fig. 5). FACS analysis revealed that trichoplein depletion increased the percentage of cells with 2n DNA (G0/G1 phase cells; Fig. 5, A and B). Immunoblotting (Fig. 5 C, top) and immunocytochemical (Fig. 5 D) analyses of cell cycle markers, including Cyclin A, also indicated a decrease of S or G2/M phase cells in response to trichoplein depletion. Furthermore, pulse-labeling experiments using BrdU to identify DNA-replicating cells showed that trichoplein knockdown reduced BrdU incorporation into nuclei (Fig. 5 D). These results strongly indicated that trichoplein depletion caused cell cycle arrest in G0/G1 phase.

To determine whether the cell cycle arrest caused in RPE1 cells by trichoplein depletion was mediated through primary cilia assembly itself, we performed simultaneous depletion of IFT-20 to abrogate formation of primary cilia (Kim et al., 2011). As shown in Fig. 5 C (bottom), the incidence of primary cilia in trichoplein-depleted cells was drastically reduced by simultaneous depletion of IFT-20. Moreover, this treatment reversed the G0/G1 arrest produced by trichoplein depletion, as assessed by analyses of FACS profiles (Fig. 5, A and B), cell cycle markers, and BrdU incorporation (Fig. 5, C and D; and Fig. S2 for another siIFT-20). In contrast, no cell cycle effects were seen in cells treated only with IFT-20 siRNA (Fig. 5, A–D; and Fig. S2). These results support the notion that trichoplein depletion causes a G0/G1 cell cycle arrest and that this arrest is mediated by the primary cilium.

We next tested whether AurA depletion also induced cilium-dependent cell cycle arrest in RPE1 cells. AurA depletion induced cell cycle arrest, but again, simultaneous depletion of IFT-20 reversed these effects (Fig. S3). Collectively, these results suggest that trichoplein and AurA cooperate to suppress primary cilia assembly, which in turn affects G1 progression.

We also examined the effects of trichoplein or AurA depletion on cell cycle progression in HeLa cells (Fig. S4). Serum starvation (not depicted) or trichoplein/AurA knockdown (Fig. S4 A) hardly induced any primary cilia formation in HeLa cells. Also, unlike in RPE1 cells (Fig. S4 C), trichoplein depletion showed almost no change in the level of Cyclin A protein (Fig. S4 B), and it had only a minor effect on the FACS profile (Fig. S4 D; Ibi et al., 2011) of HeLa cells. On the other hand, AurA knockdown produced a marked increase in Cyclin B but only a marginal change in Cyclin A in HeLa cells (Fig. S4 B). FACS analysis (Fig. S4 D) also confirmed that AurA depletion

with each siRNA, the transfection medium of Tet-FL was changed to a new growing medium with (+) or without (−) 10 ng/ml Dox. (E and F) 72 h after transfection, cells were subjected to immunoblotting with antitrichoplein (to detect both endogenous and exogenous trichoplein) or anti-GAPDH (E) or the immunofluorescence with anti-FLAG (to detect only exogenous trichoplein [Exo. Tricho.]) and anti–acetylated tubulin (F). (F, top) Magnifications of insets are shown. (E, bottom) Amounts of exogenous (exo.) or endogenous (endo.) trichoplein were quantified using densitometry, normalized to the content of GAPDH, and presented as fold of endogenous trichoplein in cells treated with control siRNA. (G) For quantification of ciliation, we analyzed 50 cells per group and then calculated the percentages of cells with primary cilia ($n = 4$). Data are means ± SD. Bars: (A [left and insets], D, and F [top]) 1 µm; (A [right] and F [bottom]) 10 µm; (C) 0.5 µm.

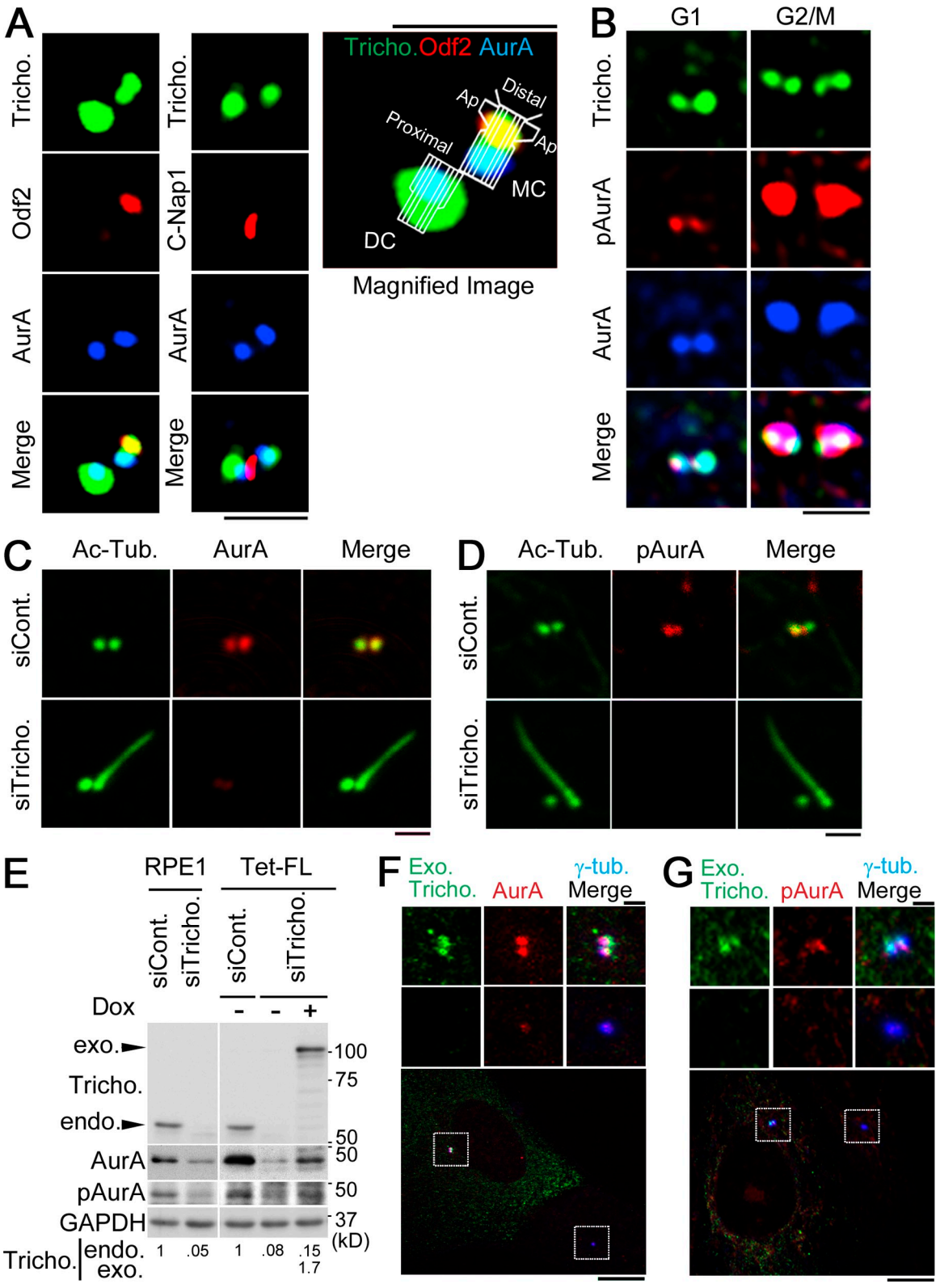

Figure 3. **Centriolar localization of trichoplein is correlated with that of AurA and Thr288–pAurA especially in G1 phase.** (A and B) RPE1 cells were subjected to the immunofluorescence staining with the indicated antibodies. MC, mother centriole; DC, daughter centriole; Ap, appendage. (C–E) Proliferating RPE1 cells were transfected with the indicated siRNA for 48 h and then subjected to immunocytochemistry (C and D) or immunoblotting (E, left; also see Fig. S1 C). The quantification data of centrosomal anti-AurA signals were shown in Fig. S1 D. siCont., control siRNA; siTricho., trichoplein siRNA; Ac-Tub., acylated tubulin. (E–G) We proceeded with the rescue experiment of endogenous (endo.) trichoplein depletion as described in the legend to Fig. 2 (E–G), with the indicated markers for additional immunoblotting (E, right), the quantification (E, bottom), and immunofluorescence (F and G). The cells were stained with anti-MBP (to detect the exogenous trichoplein [Exo. Tricho.]), anti-AurA or pAurA, and anti–γ-tubulin. Insets highlight the correlation. The quantification data of centrosomal anti-AurA and anti-pAurA signals were shown in Fig. S1 (E and F), respectively. Bars: (A–D, F [top], and G [top]) 1 µm; (F [bottom] and G [bottom]) 10 µm.

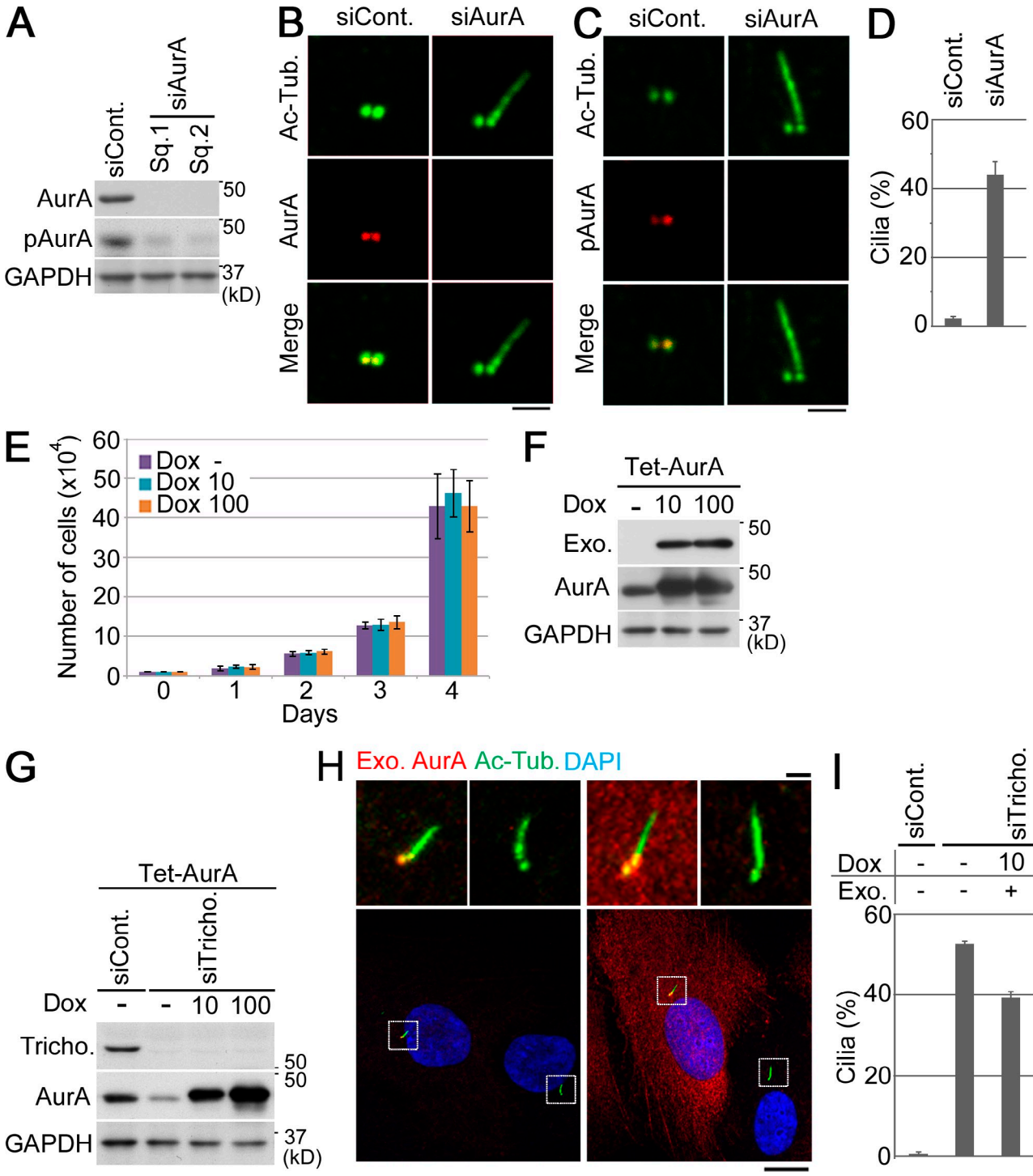

Figure 4. **Trichoplein is required for AurA activation at centrioles in G1 phase.** (A–D) Proliferating RPE1 cells were transfected with the indicated siRNA for 48 h and then subjected to immunoblotting (A) or immunocytochemistry (B and C). (E–I) Tet-ON RPE1 cells expressing Myc-AurA (Tet-AurA). (E) Little impact of exogenous AurA on the cell proliferation curve. The cells were seeded at a density of 10^4 cells per 9.6-cm^2 dish at day 0. The next day, the medium was changed to a new growing medium containing 0–100 ng/ml Dox. The medium was changed every 24 h. Data are means ± SD of three independent experiments. (F) Immunoblotting of Tet-AurA cells in E at day 4. Exogenous (Exo.) AurA was detected with anti-Myc. (G–I) Proliferating Tet-AurA cells were transfected with the indicated siRNA for 4 h. Then, the transfection medium was changed to a new growing medium containing 0–100 ng/ml Dox. The medium was changed every 24 h. (G and H) 72 h after transfection, the cells were subjected to the immunoblotting (G) or the immunocytochemistry (H). (H, top) Magnifications of the insets are shown. (D and I) The quantification of ciliation was performed as described in the legend to Fig. 2 B. siCont., control siRNA; siTricho., trichoplein siRNA; Ac-Tub., acylated tubulin. Data are means ± SD. Bars: (B, C, and H, top) 1 µm; (H, bottom) 10 µm.

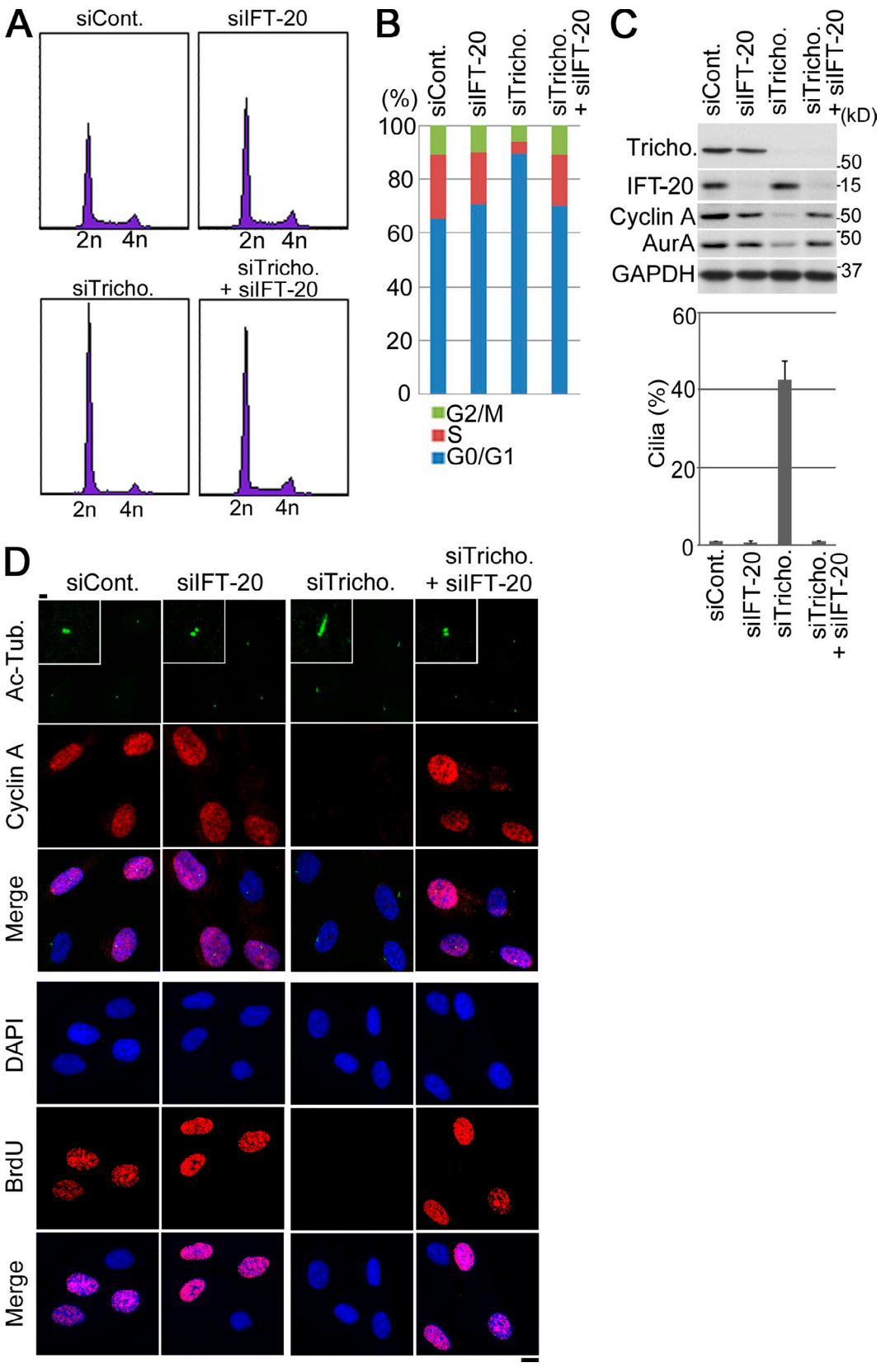

Figure 5. **Knockdown of trichoplein causes a cilium-dependent cell cycle arrest in RPE1 cells.** (A–D) Proliferating RPE1 cells were transfected with the combination of each siRNA and then subjected to FACS analysis (A and B), immunoblotting (C, top), or immunofluorescence (D). We used IFT-20 Sq. 1 in A–D; we also obtained similar results using another IFT-20 target sequence (IFT-20 Sq. 2; Fig. S2). (C, bottom) The percentage of cells with primary cilia was calculated as described in the legend to Fig. 2 B. Data are means ± SD. (D) Insets indicate higher magnifications. siCont., control siRNA; siTricho., trichoplein siRNA; Ac-Tub., acylated tubulin. Bars: (D, insets) 1 µm; (D, main images) 10 µm.

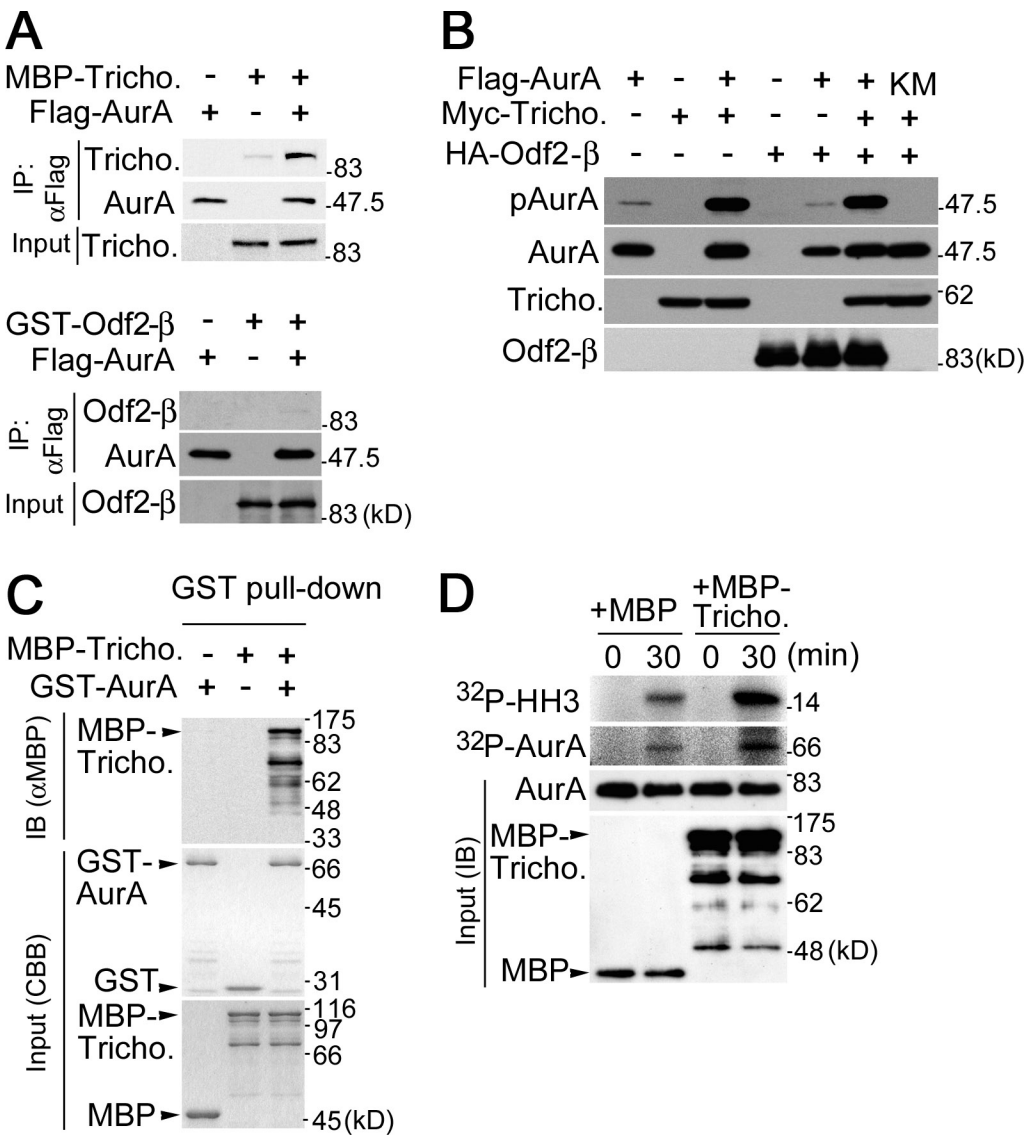

Figure 6. **Trichoplein binds and activates AurA.** (A) AurA can bind trichoplein but not Odf2-β in HeLa cells. The cells were transfected with the indicated proteins. 24 h after the transfection, cell extracts were subjected to immunoprecipitation with anti-Flag. Before immunoprecipitation, a fraction of each cell extract was subjected to immunoblotting with anti-MBP (trichoplein) or anti-GST (Odf2-β) as an input. (B) AurA can be activated by trichoplein in HeLa cells. The cells were transfected with Flag-tagged AurA wild type or its kinase-dead mutant (KM) in addition to Myc-tagged trichoplein and/or HA-tagged Odf2-β. 24 h after transfection, cell lysates were subjected to immunoblotting with anti-pAurA, anti-Flag (AurA), anti-Myc (trichoplein), or anti-HA (Odf2-β). (C) AurA can directly bind trichoplein in vitro. GST pull-down assays were performed using the indicated purified proteins. GST or MBP was used as a negative control (−). (D) AurA can be directly activated by trichoplein in vitro. The kinase assays were performed as described in Materials and methods. Each reaction mixture was subjected to autoradiography (^{32}P-H3 or ^{32}P-AurA) or immunoblotting with anti-GST (AurA) or anti-MBP (MBP or MBP-trichoplein). CBB, Coomassie brilliant blue; IP, immunoprecipitation; Tricho., trichoplein; IB, immunoblot.

increased the G2/M population. Together with the data showing that trichoplein or AurA knockdown induced G0/G1 arrest in RPE1 cells, these results further support the notion that trichoplein and AurA control cell cycle progression indirectly, that is, through the suppression of primary cilia assembly in G1 phase. We conclude that the observed cell cycle regulatory impact of trichoplein and AurA depends on the ability of cells to form primary cilia.

Trichoplein activates AurA specifically at the centriole

To examine a possible interaction of trichoplein with AurA, we tested whether the two proteins bind each other in cells. As shown in Fig. 6 A, MBP-tagged trichoplein was able to interact with Flag-tagged AurA in anti-Flag immunoprecipitation experiments. Another known binding partner of trichoplein, Odf2-β (Ibi et al., 2011), was not detected in these immunoprecipitates, arguing against the formation of a ternary complex between these proteins. Importantly, coexpression of trichoplein and AurA enhanced AurA autophosphorylation at Thr288 (Fig. 6 B, pAurA), indicating that trichoplein binding caused the activation of AurA (Walter et al., 2000). Although Odf2-β could bind trichoplein directly (Ibi et al., 2011), Odf2-β appeared to have little impact on AurA activation by trichoplein (Fig. 6 B). We next purified GST-AurA from insect cells and MBP-trichoplein from *Escherichia coli*. GST pull-down assays using these recombinant proteins revealed that GST-AurA

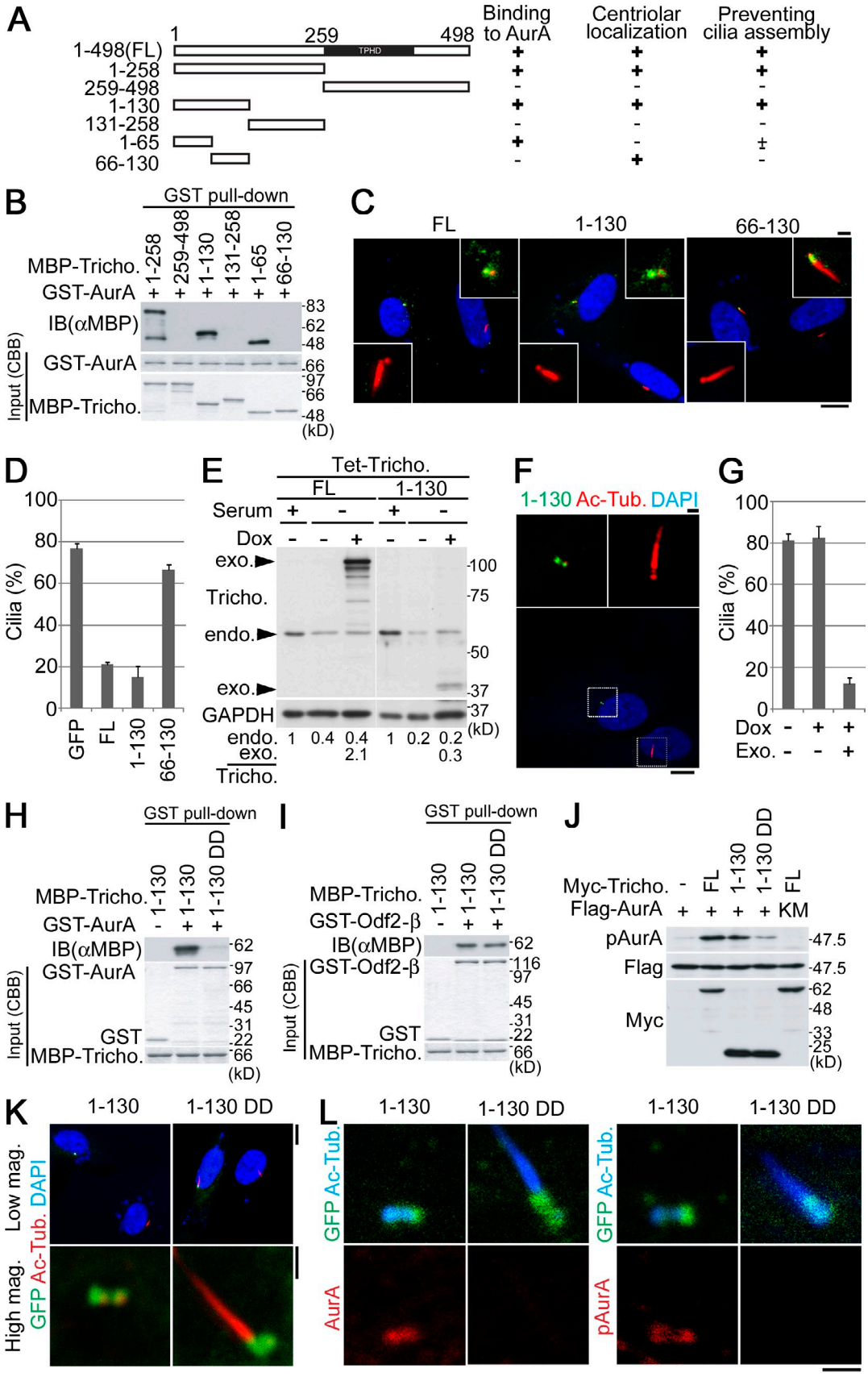

Figure 7. **The binding of trichoplein to AurA in centrioles is indispensable for suppression of primary cilia assembly.** (A–D) Schematic (A) of human trichoplein full length (FL) and deletion constructs showing the ability to bind AurA (B), to localize to the centriole (C), and to prevent primary cilia assembly (C and D). Numbers indicate human trichoplein amino acids. TPHD indicates a trichohyalin and plectin homology domain in trichoplein. (B) Interactions

readily bound MBP-trichoplein, although GST alone did not bind, and conversely, GST-AurA did not bind the MBP tag (Fig. 6 C). As shown in Fig. 6 D, trichoplein enhanced AurA in vitro kinase activity toward both histone H3 and AurA itself. These results suggest that trichoplein can directly bind and activate AurA.

Trichoplein was originally identified as a keratin scaffold protein (Nishizawa et al., 2005; Ibi et al., 2011), but it is also known as mitostatin, for which multiple functions and localizations have been previously described (Vecchione et al., 2009; Cerqua et al., 2010). Thus, we asked whether the trichoplein function described here is centriole specific. We prepared several trichoplein mutants and characterized these for their ability to bind AurA, localize to centrioles, and inhibit cilia assembly (summarized in Fig. 7 A). Based on GST pull-down assays using MBP-tagged trichoplein deletion mutants, we found that at least the first 65 residues of trichoplein (1–65) are necessary to bind AurA (Fig. 7, A and B). By expressing the mutants as GFP fusion proteins in RPE1 cells, we found further that at least residues 66–130 are necessary for localization to the centriole (Fig. 7, A and C; and Fig. S5 A). Collectively, we show that the transient expression of a trichoplein fragment spanning residues 1–130 (referred to as 1–130) is necessary and sufficient for centriolar localization and function: immunofluorescence microscopy demonstrates the specific localization of this mutant to centrioles, with little staining of other cytoplasmic structures, such as keratin IFs and/or mitochondria, and it also illustrates the ability of this mutant to suppress primary cilia formation in serum-starved RPE1 cells (Fig. 7, A, C, and D; and Fig. S5 A).

To further confirm the centriole specificity of trichoplein function, we established a stable Tet-ON RPE1 cell line expressing 1–130 (Tet-1–130). As shown in Fig. 7 (E–G), expression of 1–130 prevented primary cilia assembly in serum-starved cells. Likewise, upon cultivation with serum, ciliary assembly triggered by trichoplein depletion was suppressed by expression of 1–130 (Fig. S5, B–D). Under both experimental conditions, 1–130 worked at much lower expression levels than FL or endogenous trichoplein (Fig. 2 E, Fig. 7 E, and Fig. S5 B), which is consistent with the immunofluorescence data indicating that 1–130 localizes more specifically to centrioles than FL trichoplein (Fig. 7 F).

To elucidate the importance of trichoplein binding to AurA, we designed mutations that reduce the ability of trichoplein to bind AurA. Based on our data (Fig. 7, A and B) and a previous study regarding the interaction of TPX2 with AurA (Bayliss et al., 2004), we constructed a 1–130 protein carrying Ala52 and Trp54 mutated to Asp (referred to as 1–130DD; Fig. S5 E). Compared with 1–130, 1–130DD reduced the binding activity to AurA (Fig. 7 H) but not to Odf2-β (Fig. 7 I). 1–130DD had also less AurA activation activity than 1–130 or FL (Fig. 7 J). Importantly, 1–130DD lost not only the ability to activate AurA at the centrioles but also to suppress primary cilia formation in serum-starved RPE1 cells, whereas 1–130DD could localize to the centriole like 1–130 (Fig. 7, K and L). Collectively, these results suggest that trichoplein controls AurA activation at the centriole, which in turn is required for the suppression of unscheduled primary cilia formation in G1 phase.

Discussion

In the present study, we provide evidence for a novel function of trichoplein and AurA in the suppression of primary cilia formation in G1 phase. This conclusion is based on the following findings: First, trichoplein localizes to centrioles but disappears from basal bodies (Fig. 1, A and B). Second, primary cilia assembly is suppressed by exogenous trichoplein expression (Fig. 1, C and D). Third, ciliogenesis is induced by RNAi-mediated trichoplein depletion (Fig. 2). Fourth, AurA cooperates with trichoplein in the suppression of primary cilia formation (Fig. 3, Fig. 4, Fig. 6, and Fig. 7). Fifth, trichoplein depletion from RPE1 cells leads to G0/G1 arrest in a cilium-dependent manner (Fig. 5). These data lead us to propose the following model: trichoplein activates AurA likely through a direct molecular interaction at G1-phase centrioles. This activation suppresses the assembly of a new ciliary axoneme at the mother centriole. Like the promotion of ciliary disassembly at the G0/G1 transition (Pugacheva et al., 2007), this suppression may be mediated by AurA-induced phosphorylation and activation of HDAC-6. Regardless of the precise mechanism, we propose that the lack of AurA activation by trichoplein at centrioles induces primary cilia formation, which then causes cellular quiescence.

Cell cycle progression shows an inverse relationship with ciliation (Mikule et al., 2007). Thus, by abrogating primary

were determined by GST pull-down assays using each purified protein. (C and D) Centriolar localization and primary cilia inhibition (also see Fig. S5 A) were tested as follows. RPE1 cells were transiently transfected with each GFP fusion protein. 3 h after transfection, the medium was changed to serum-free medium. (C) Cells were incubated for additional 48 h and then subjected to the immunostaining with anti–acetylated tubulin (red) or anti–γ-tubulin (not depicted). Exogenous trichoplein FL and deletion mutants were visualized by GFP luminescence (green). Nuclei were also stained with DAPI (blue). Higher magnification images of centrioles with or without detectable GFP luminescence are indicated in top right or bottom left insets, respectively. (D) To quantify data shown in C, we analyzed 100 GFP-positive cells per group and calculated the percentages of cells with primary cilia (n = 3). (E–G) Each Tet-ON RPE1 cell line was incubated as described in the legend to Fig. 1 (C and D) and then subjected to immunoblotting (E) and the quantification (E, bottom; as described in Fig. 2 E), with a slight modification. (F) 10 ng/ml Dox was used for the induction of the GFP-trichoplein 1–130 fragment, which was visualized by GFP luminescence (green). (top) Magnifications of insets are shown. (G) The quantification data were obtained as described in the legend to Fig. 1 D. (H and I) GST pull-down assays using GST-AurA (H) or –Odf2-β (I) in the presence of purified 1–130 or 1-130DD (Fig. S5 E) in vitro. As a negative control, GST was used instead of each GST-tagged protein (−). (J) HeLa cells were transfected with Flag-tagged AurA wildtype (+) or a kinase-dead mutant (KM) in the presence of Myc-tagged trichoplein FL, 1–130, or 1-130DD as described in the legend of Fig. 6 B. (K and L) AurA recruitment/activation and primary cilia inhibition were tested by expression of each trichoplein 1–130 fragment as a GFP fusion in RPE1 cells. The cells were transiently transfected and incubated as described in A–D. Then, the cells were immunostained with anti–acetylated tubulin (Ac-Tub.). Cells were simultaneously stained with DAPI (K), anti-AurA (L, left), or anti-pAurA (L, right). Tricho., trichoplein; IB, immunoblot; CBB, Coomassie brilliant blue; exo., exogenous; endo., endogenous; mag., magnification. Data are means ± SD. Bars: (C [main images], F [bottom], and K [top]) 10 µm; (C [insets], F [top], K [bottom], and L) 1 µm.

cilia, we tried to clarify the relationship between the block to ciliary assembly by the trichoplein–AurA pathway and cell cycle progression. As IFT-20 is required for ciliogenesis but not cell cycle progression (Baker et al., 2003; Follit et al., 2006), we abrogated primary cilia by codepletion of IFT-20 (Kim et al., 2011) with trichoplein. As a result of IFT-20 depletion, both phenotypes of trichoplein depletion in RPE1 cells were overcome: not only was primary cilia formation suppressed, but a release from the G0/G1 arrest was also triggered (Fig. 5 and Fig. S2). This clearly shows that primary cilia play an active role in blocking cell proliferation.

To exclude possible effects unrelated to cilia, we have abrogated primary cilia through three different routes, notably chloral hydrate treatment (unpublished data) and the codepletion of trichoplein with IFT-88 (unpublished data) or IFT-20 (this study). It should be noted that each experiment potentially contains a risk for extraciliary effects: chloral hydrate disrupts mitosis (Lee et al., 1987), the knockdown of IFT-88 promotes cell cycle progression to S and G2/M phases in nonciliated HeLa cells (Robert et al., 2007), and IFT-20 is also known as a Golgi protein (Follit et al., 2006). But, RPE1 cells treated with each method alone showed a profile similar to nontreated cells. Although we recognize potential technical limitations, the consistency of the results obtained using three independent methods, combined with control experiments, makes us confident to conclude that primary cilia play an active role in regulating cell proliferation through the trichoplein–AurA pathway.

Remarkably, the knockdown of trichoplein or AurA could not induce G1 arrest in HeLa cells (Fig. S4). This is not necessarily surprising, as primary cilia formation is rarely, if ever, observed upon serum starvation of these tumor cells. These data support our conclusion that the trichoplein–AurA pathway does not directly control the G1 progression machinery. Instead, it continuously suppresses primary cilia assembly in RPE1 cells, which in turn is required to allow G1 progression.

It has been reported that the ectopic expression of trichoplein/mitostatin in prostate cancer cells reduces cell proliferation (Fassan et al., 2011). On the surface, this result contrasts with our observation that knockdown of trichoplein arrests cell proliferation in RPE1 cells. However, we note that cancer cell lines differ markedly from nontransformed cells in their ability to form cilia and that different cancer cell lines often display different behavior among themselves, including differences in signal transduction systems.

AurA was originally discovered in a screen for *Drosophila melanogaster* mutations affecting the poles of the mitotic spindle (Glover et al., 1995), and many AurA functions are related to mitosis (Carmena et al., 2009). These mitotic functions largely depend on AurA-associated proteins, the disruption or depletion of which induces mitotic disorders, such as the failure of centrosome maturation, centrosome separation, and bipolar spindle formation (Carmena et al., 2009). However, trichoplein depletion shows no apparent mitotic phenotypes, whereas AurA depletion shows mitotic phenotypes, especially in HeLa cells in which primary cilia are not assembled in response to cultivation in serum-free medium (Fig. S4 and not depicted). In addition, AurA activation is not restricted to subcellular areas where trichoplein localizes (Fig. 3 B and Fig. S1 A). Hence, we consider it likely that trichoplein is dispensable for mitotic AurA activation and function. Rather, we propose that trichoplein activates AurA predominantly in G1 phase.

Together with trichoplein, HEF1 (Pugacheva et al., 2007) and Pifo (Kinzel et al., 2010) also modulate nonmitotic AurA activation. These proteins stimulate HDAC-6–dependent tubulin deacetylation and destabilize the ciliary axoneme (Pugacheva et al., 2007). However, HEF1 (Pugacheva and Golemis, 2005) and Pifo (Kinzel et al., 2010) also play important roles in mitosis. Whereas the extent of Pifo regulation during the cell cycle remains largely unknown, trichoplein clearly shows characteristics that distinguish it from HEF1. Trichoplein localizes to centrioles throughout the cell cycle but disappears from basal bodies, whereas HEF1 is transiently expressed at the G0/G1 and G2/M transitions (Pugacheva et al., 2007). These observations raise the possibility that HEF1 participates in ciliary resorption at the G0/G1 transition and that trichoplein then suppresses primary cilia assembly through the subsequent G1 phase. This continuous suppression of cilia formation by trichoplein is then required for cell cycle progression from G1 to S phase.

We previously reported that trichoplein interacts with several proteins, such as keratin IFs (Nishizawa et al., 2005), Odf2, and ninein (Ibi et al., 2011). Here, we have presented evidence for a functional role of the trichoplein–AurA interaction specifically in the suppression of primary cilia assembly, which is necessary for G1 progression. Thus, in proliferating cells, trichoplein serves as a hub not only for appendage-associated ninein involved in MT anchoring at the mother centriole (Ibi et al., 2011) but also for centriole-associated AurA implicated in the destabilization of the ciliary axoneme (this study). On the other hand, in differentiated, nondividing epithelial cells, trichoplein is translocated from centrioles to keratin IFs and desmosomes (Nishizawa et al., 2005; Ibi et al., 2011). The aforementioned observations raise the question of how trichoplein changes its binding partners and localization. This question will be addressed in the future.

Materials and methods

Cell culture

RPE1 (human telomerase reverse transcriptase–immortalized retinal pigment epithelia; CRL-4000; American Type Culture Collection) or HeLa (human cervical carcinoma) cells were grown in DME/F12 (a 1:1 mixture of DME and Ham's F12 medium; Invitrogen) or DME supplemented with 10% FBS, respectively. We established Tet-ON RPE1 cells in which MBP-trichoplein-3×Flag, GFP-trichoplein 1–130, or Myc-AurA is expressed in a tetracycline/Dox-dependent manner (Ibi et al., 2011). For the observation of primary cilia formation, RPE1 cells were cultured in a serum-free medium for 48 h. In all experiments, cells were maintained at <100% of the confluence to avoid ciliogenesis caused by the contact inhibition.

Materials

We prepared polyclonal rabbit antitrichoplein antibody (Nishizawa et al., 2005; Ibi et al., 2011) and mouse monoclonal anti-AurA–phospho-Thr288 (Ohashi et al., 2006) as previously described. The rabbit anti–IFT-88 antibody was a gift from B.K. Yoder (University of Alabama, Birmingham, AL). H. Saya (Keio University, Shinjuku-ku, Tokyo, Japan) provided the AurA-related constructs. Antibodies from commercial sources were obtained as follows: anti–Centrin 2 (N-17; Santa Cruz Biotechnology, Inc.); anti–acetylated tubulin (6-11B-1), anti-Odf2, anti-Flag (M2), or anti–γ-tubulin (T3559;

Sigma-Aldrich); anti–C-Nap1 (clone 42), anti-AurA (clone 4), anti–Cyclin A, or anti–Cyclin B (BD); anti-Myc (9E10) or anti-HA (12CA5; Roche); anti-GST or anti-p38 MAPK (Cell Signaling Technology); anti-MBP (ab9385; New England Biolabs, Inc.); anti–γ-tubulin (TU-30) and HRP-conjugated anti–glyceraldehyde 3-phosphate dehydrogenase (GAPDH; Abcam); anti–IFT-20 (Proteintech Group); and anti-Myc (4A6; Millipore). Species-specific secondary antibodies were conjugated to Alexa Fluor 488, 555, and 647 (Invitrogen). Western blot analyses were performed as described previously (Sugimoto et al., 2008; Enomoto et al., 2009).

Transfection with siRNAs or plasmids

The following 21-nucleotide double-strand RNAs were purchased from QIAGEN or Invitrogen: trichoplein target sequence 1 (Sq. 1), 5′-(AA)GGCAGAATGGAGCTCTAAA-3′; trichoplein Sq. 2, 5′-(CA)GGGCATTGTTCCATGGTTA-3′; AurA Sq. 1, 5′-(TC)CCAGCGCATTCCTTTGCAA-3′; AurA Sq. 2, 5′-(CA)CCTTCGGCATCCTAATATT-3′; IFT-20 Sq. 1, 5′-(CA)GCAACTTCAAGCCCTAATA-3′; and IFT-20 Sq. 2, 5′-(CA)GAAAATAGTTGGTGGTTTA-3′. The parentheses indicate the place where the complementary overhang of the antisense associated. Select negative control #2 siRNA (Silencer; Invitrogen) or negative control siRNA (catalogue no. 1027310; QIAGEN) was used as a negative control. In all transfections, RPE1 or HeLa cells were exponentially growing. They were transfected with each siRNA as described previously (Ibi et al., 2011). Transfection with plasmids was also performed as described previously (Ibi et al., 2011).

Immunofluorescence microscopy

Cultured cells were grown on coverslips (Iwaki Glass Co., Ltd.). The fixations with methanol or formaldehyde were performed as described previously (Sugimoto et al., 2008) with slight modifications. For the immunostaining with anti–acetylated tubulin, cells were incubated for 15 min on ice before fixation. For the immunostaining with anti-AurA or pAurA, cells were treated with methanol at −20°C for 10 min and then with 0.01% saponin in PBS at room temperature for 15 min. For the immunostaining with anti–Cyclin A or the observation of GFP fusion protein, cells were fixed with 1% formaldehyde in PBS for 15 min and then permeabilized with PBS containing 0.2% Triton X-100 for 15 min. Then, they were blocked with 1% BSA/PBS for 15 min and incubated with primary antibodies. After being washed with PBS three times, samples were incubated for 30 min with secondary antibodies. Using the DNA replication assay kit (Millipore), we judged cells undergoing DNA replication through the detection of BrdU uptake in the nuclei. Fluorescence images in Fig. 1 A and Fig. 3 (A and B) were obtained by using the DeltaVision system (Applied Precision), as previously described (Ishikawa et al., 2005), equipped with a microscope (IX70; Olympus), a Plan Apochromat 100×/1.40 NA oil immersion lens (Olympus), and a cooled charge-coupled device camera (CoolSNAP HQ; Photometrics). The images were obtained with 0.2-µm intervals in a z section, deconvolved, and integrated with softWoRx software (Applied Precision). Other images were obtained by confocal microscopy (LSM 510 META; Carl Zeiss) equipped with a microscope (Axiovert 200 M; Carl Zeiss), a Plan Apochromat 100×/1.4 NA oil immersion lens, a Plan Apochromat 150×/1.35 NA glycerol immersion lens, and LSM Image Browser software (Carl Zeiss) as previously described (Sugimoto et al., 2008). Images were taken at room temperature and further processed using Photoshop Elements 6.0 (Adobe) according to *The Journal of Cell Biology* guidelines.

Transmission electron microscopy

RPE1 cells cultured on coverslips were fixed with 2% fresh formaldehyde and 2.5% glutaraldehyde in 0.1 M sodium cacodylate buffer, pH 7.4, for 2 h at room temperature. After washing with 0.1 M cacodylate buffer, pH 7.4, they were postfixed with ice-cold 1% OsO_4 in the same buffer for 2 h. The samples were rinsed with distilled water, stained with 0.5% aqueous uranyl acetate for 2 h or overnight at room temperature, dehydrated with ethanol and propylene oxide, and embedded in an embedding kit (Poly/Bed 812; PolySciences, Inc.). After removal of coverslips using ice-cold hydrofluoric acid, ultra thin sections were cut, doubly stained with uranyl acetate and Reynolds's lead citrate, and viewed with a transmission electron microscope (JEM-1010; JEOL) with a charge-coupled device camera (BioScan model 792; Gatan, Inc.) at an accelerating voltage of 100 kV.

Immunoprecipitation

We performed the immunoprecipitation using anti-Flag M2 affinity gel (Sigma-Aldrich) according to the manufacturer's protocol.

Preparation of recombinant proteins

MBP-tagged trichoplein and deletion mutants were expressed in BL21-CodonPlus-RP (Agilent Technologies) transformed with pMAL (New England Biolabs, Inc.) carrying each protein. We generated the recombinant baculoviruses encoding GST-AurA and GST–Odf2-β, as previously described (Ibi et al., 2011), by the combination of vector conversion system (Gateway; Invitrogen) and baculovirus expression system (Bac-to-Bac; Invitrogen). Then, GST-AurA and GST–Odf2-β were expressed in the baculovirus-infected Sf9 cells. Each MBP or GST fusion protein was purified through the affinity chromatography with the amylose resin (New England Biolabs, Inc.) or with glutathione–Sepharose 4B (GE Healthcare), respectively.

GST pull-down assay

10 µg GST, GST-AurA, or GST–Odf2-β protein was preincubated with 10 µl glutathione–Sepharose 4B in binding buffer (50 mM Tris-Cl, pH 7.5, 150 mM NaCl, 1% TritonX-100, 1 mM EDTA, and protease inhibitor cocktail [Nacalai Tesque, Inc.]) for 1 h at 4°C. After washing with binding buffer three times, the beads were incubated with 10 µg MBP or each MBP fusion protein in 200 µl of the binding buffer for 1 h at 4°C. After washing with binding buffer three times, the beads were subjected to immunoblotting with anti-MBP.

In vitro kinase assay

100 nM GST-AurA was preincubated with MBP or MBP-trichoplein (500 nM each) in 20 ml of the reaction buffer (25 mM Tris-Cl, pH 7.5, 10 mM $MgCl_2$, and 100 µM ATP) for 30 min at 30°C. 2 µl of the premixture (10 nM GST-AurA and 50 nM MBP-related protein) was incubated in 20 µl of the reaction buffer with 300 nM histone H3 (Roche) and 5 µCi γ-[^{32}P]ATP for 0 or 30 min.

FACS analysis

FACS analyses that show the DNA content in each group were performed similarly to a previous study (Matsuyama et al., 2011) as follows. Approximately 10^6 cells were collected by trypsinization, resuspended in buffer solution (Cycletest Plus kit; BD), and stored at −80°C. Then, we treated them according to the manufacturer's protocol (Cycletest Plus kit) and analyzed them using a FACScan (BD) and CellQuest software (BD).

Online supplemental material

Fig. S1 shows that knockdown of trichoplein reduces total and centrosomal levels of AurA and pAurA. Fig. S2 shows that cell cycle arrest by trichoplein depletion is alleviated by codepletion of IFT-20 with Sq. 2. Fig. S3 shows that knockdown of AurA causes a cilium-dependent cell cycle arrest in RPE1 cells. Fig. S4 shows that knockdown of trichoplein or AurA shows different phenotypes in HeLa cells. Fig. S5 shows that ciliation induced by trichoplein depletion is rescued by the centriole-specific expression of the trichoplein truncation mutant 1–130. Online supplemental material is available at http://www.jcb.org/cgi/content/full/jcb.201106101/DC1.

We are grateful to H. Saya for providing AurA-related constructs, B.K. Yoder for the anti-Polaris/IFT-88 antibody, S. Tsukita for helpful discussions, P. Li, Z. Wang, P. Zou, C. Yuhara, and K. Kobori for technical assistance, Y. Takada for secretarial expertise, J. Shields for critical reading of the manuscript, and E. Nigg for critical comments on the language and the organization throughout the manuscript.

This work was supported in part by Grants-in-Aid for Scientific Research from the Japan Society for the Promotion of Science and from the Ministry of Education, Science, Technology, Sports and Culture of Japan, by a Grant-in-Aid for the Third-Term Comprehensive 10-Year Strategy for Cancer Control from the Ministry of Health and Welfare (Japan), by the Uehara Memorial Foundation, by the Astellas Foundation for Research on Metabolic Disorders, by the Naito Foundation, by the Takeda Science Foundation, and by the Daiichi Sankyo Foundation of Life Science.

Submitted: 16 June 2011
Accepted: 22 March 2012

References

Anderson, C.T., A.B. Castillo, S.A. Brugmann, J.A. Helms, C.R. Jacobs, and T. Stearns. 2008. Primary cilia: cellular sensors for the skeleton. *Anat. Rec. (Hoboken).* 291:1074–1078. http://dx.doi.org/10.1002/ar.20754

Baker, S.A., K. Freeman, K. Luby-Phelps, G.J. Pazour, and J.C. Besharse. 2003. IFT20 links kinesin II with a mammalian intraflagellar transport complex that is conserved in motile flagella and sensory cilia. *J. Biol. Chem.* 278:34211–34218. http://dx.doi.org/10.1074/jbc.M300156200

Bayliss, R., T. Sardon, J. Ebert, D. Lindner, I. Vernos, and E. Conti. 2004. Determinants for Aurora-A activation and Aurora-B discrimination by TPX2. *Cell Cycle*. 3:402–407. http://dx.doi.org/10.4161/cc.3.4.777

Berbari, N.F., A.K. O'Connor, C.J. Haycraft, and B.K. Yoder. 2009. The primary cilium as a complex signaling center. *Curr. Biol.* 19:R526–R535. http://dx.doi.org/10.1016/j.cub.2009.05.025

Bettencourt-Dias, M., and D.M. Glover. 2007. Centrosome biogenesis and function: centrosomics brings new understanding. *Nat. Rev. Mol. Cell Biol.* 8:451–463. http://dx.doi.org/10.1038/nrm2180

Bornens, M. 2008. Organelle positioning and cell polarity. *Nat. Rev. Mol. Cell Biol.* 9:874–886. http://dx.doi.org/10.1038/nrm2524

Carmena, M., S. Ruchaud, and W.C. Earnshaw. 2009. Making the Auroras glow: regulation of Aurora A and B kinase function by interacting proteins. *Curr. Opin. Cell Biol.* 21:796–805. http://dx.doi.org/10.1016/j.ceb.2009.09.008

Cerqua, C., V. Anesti, A. Pyakurel, D. Liu, D. Naon, G. Wiche, R. Baffa, K.S. Dimmer, and L. Scorrano. 2010. Trichoplein/mitostatin regulates endoplasmic reticulum-mitochondria juxtaposition. *EMBO Rep.* 11:854–860. http://dx.doi.org/10.1038/embor.2010.151

Eggenschwiler, J.T., and K.V. Anderson. 2007. Cilia and developmental signaling. *Annu. Rev. Cell Dev. Biol.* 23:345–373. http://dx.doi.org/10.1146/annurev.cellbio.23.090506.123249

Ehler, L.L., J.A. Holmes, and S.K. Dutcher. 1995. Loss of spatial control of the mitotic spindle apparatus in a *Chlamydomonas reinhardtii* mutant strain lacking basal bodies. *Genetics*. 141:945–960.

Enomoto, M., H. Goto, Y. Tomono, K. Kasahara, K. Tsujimura, T. Kiyono, and M. Inagaki. 2009. Novel positive feedback loop between Cdk1 and Chk1 in the nucleus during G2/M transition. *J. Biol. Chem.* 284:34223–34230. http://dx.doi.org/10.1074/jbc.C109.051540

Fassan, M., D. D'Arca, J. Letko, A. Vecchione, M.P. Gardiman, P. McCue, B. Wildemore, M. Rugge, D. Shupp-Byrne, L.G. Gomella, et al. 2011. Mitostatin is down-regulated in human prostate cancer and suppresses the invasive phenotype of prostate cancer cells. *PLoS ONE*. 6:e19771. http://dx.doi.org/10.1371/journal.pone.0019771

Follit, J.A., R.A. Tuft, K.E. Fogarty, and G.J. Pazour. 2006. The intraflagellar transport protein IFT20 is associated with the Golgi complex and is required for cilia assembly. *Mol. Biol. Cell*. 17:3781–3792. http://dx.doi.org/10.1091/mbc.E06-02-0133

Fry, A.M., T. Mayor, P. Meraldi, Y.D. Stierhof, K. Tanaka, and E.A. Nigg. 1998. C-Nap1, a novel centrosomal coiled-coil protein and candidate substrate of the cell cycle–regulated protein kinase Nek2. *J. Cell Biol.* 141:1563–1574. http://dx.doi.org/10.1083/jcb.141.7.1563

Gerdes, J.M., E.E. Davis, and N. Katsanis. 2009. The vertebrate primary cilium in development, homeostasis, and disease. *Cell*. 137:32–45. http://dx.doi.org/10.1016/j.cell.2009.03.023

Glover, D.M., M.H. Leibowitz, D.A. McLean, and H. Parry. 1995. Mutations in aurora prevent centrosome separation leading to the formation of monopolar spindles. *Cell*. 81:95–105. http://dx.doi.org/10.1016/0092-8674(95)90374-7

Ibi, M., P. Zou, A. Inoko, T. Shiromizu, M. Matsuyama, Y. Hayashi, M. Enomoto, D. Mori, S. Hirotsune, T. Kiyono, et al. 2011. Trichoplein controls microtubule anchoring at the centrosome by binding to Odf2 and ninein. *J. Cell Sci.* 124:857–864. http://dx.doi.org/10.1242/jcs.075705

Ishikawa, H., and W.F. Marshall. 2011. Ciliogenesis: building the cell's antenna. *Nat. Rev. Mol. Cell Biol.* 12:222–234. http://dx.doi.org/10.1038/nrm3085

Ishikawa, H., A. Kubo, S. Tsukita, and S. Tsukita. 2005. Odf2-deficient mother centrioles lack distal/subdistal appendages and the ability to generate primary cilia. *Nat. Cell Biol.* 7:517–524. http://dx.doi.org/10.1038/ncb1251

Jantscher, F., C. Pirker, C.E. Mayer, W. Berger, and H. Sutterluety. 2011. Overexpression of Aurora-A in primary cells interferes with S-phase entry by diminishing Cyclin D1 dependent activities. *Mol. Cancer*. 10:28. http://dx.doi.org/10.1186/1476-4598-10-28

Keller, L.C., S. Geimer, E. Romijn, J. Yates III, I. Zamora, and W.F. Marshall. 2009. Molecular architecture of the centriole proteome: the conserved WD40 domain protein POC1 is required for centriole duplication and length control. *Mol. Biol. Cell*. 20:1150–1166. http://dx.doi.org/10.1091/mbc.E08-06-0619

Kim, S., N.A. Zaghloul, E. Bubenshchikova, E.C. Oh, S. Rankin, N. Katsanis, T. Obara, and L. Tsiokas. 2011. Nde1-mediated inhibition of ciliogenesis affects cell cycle re-entry. *Nat. Cell Biol.* 13:351–360. http://dx.doi.org/10.1038/ncb2183

Kinzel, D., K. Boldt, E.E. Davis, I. Burtscher, D. Trümbach, B. Diplas, T. Attié-Bitach, W. Wurst, N. Katsanis, M. Ueffing, and H. Lickert. 2010. Pitchfork regulates primary cilia disassembly and left-right asymmetry. *Dev. Cell*. 19:66–77. http://dx.doi.org/10.1016/j.devcel.2010.06.005

Kobayashi, T., and B.D. Dynlacht. 2011. Regulating the transition from centriole to basal body. *J. Cell Biol.* 193:435–444. http://dx.doi.org/10.1083/jcb.201101005

Laoukili, J., E. Perret, S. Middendorp, O. Houcine, C. Guennou, F. Marano, M. Bornens, and F. Tournier. 2000. Differential expression and cellular distribution of centrin isoforms during human ciliated cell differentiation in vitro. *J. Cell Sci.* 113:1355–1364.

Lee, G.M., J. Diguiseppi, G.M. Gawdi, and B. Herman. 1987. Chloral hydrate disrupts mitosis by increasing intracellular free calcium. *J. Cell Sci.* 88:603–612.

Matsuyama, M., H. Goto, K. Kasahara, Y. Kawakami, M. Nakanishi, T. Kiyono, N. Goshima, and M. Inagaki. 2011. Nuclear Chk1 prevents premature mitotic entry. *J. Cell Sci.* 124:2113–2119. http://dx.doi.org/10.1242/jcs.086488

Mayor, T., Y.D. Stierhof, K. Tanaka, A.M. Fry, and E.A. Nigg. 2000. The centrosomal protein C-Nap1 is required for cell cycle–regulated centrosome cohesion. *J. Cell Biol.* 151:837–846. http://dx.doi.org/10.1083/jcb.151.4.837

Mikule, K., B. Delaval, P. Kaldis, A. Jurcyzk, P. Hergert, and S. Doxsey. 2007. Loss of centrosome integrity induces p38-p53-p21-dependent G1-S arrest. *Nat. Cell Biol.* 9:160–170. http://dx.doi.org/10.1038/ncb1529

Nigg, E.A. 2001. Mitotic kinases as regulators of cell division and its checkpoints. *Nat. Rev. Mol. Cell Biol.* 2:21–32. http://dx.doi.org/10.1038/35048096

Nigg, E.A., and J.W. Raff. 2009. Centrioles, centrosomes, and cilia in health and disease. *Cell*. 139:663–678. http://dx.doi.org/10.1016/j.cell.2009.10.036

Nishizawa, M., I. Izawa, A. Inoko, Y. Hayashi, K. Nagata, T. Yokoyama, J. Usukura, and M. Inagaki. 2005. Identification of trichoplein, a novel keratin filament-binding protein. *J. Cell Sci.* 118:1081–1090. http://dx.doi.org/10.1242/jcs.01667

Ohashi, S., G. Sakashita, R. Ban, M. Nagasawa, H. Matsuzaki, Y. Murata, H. Taniguchi, H. Shima, K. Furukawa, and T. Urano. 2006. Phospho-regulation of human protein kinase Aurora-A: analysis using anti-phospho-Thr288 monoclonal antibodies. *Oncogene*. 25:7691–7702. http://dx.doi.org/10.1038/sj.onc.1209754

Pan, J., Q. Wang, and W.J. Snell. 2004. An aurora kinase is essential for flagellar disassembly in *Chlamydomonas*. *Dev. Cell*. 6:445–451. http://dx.doi.org/10.1016/S1534-5807(04)00064-4

Paoletti, A., M. Moudjou, M. Paintrand, J.L. Salisbury, and M. Bornens. 1996. Most of centrin in animal cells is not centrosome-associated and centrosomal centrin is confined to the distal lumen of centrioles. *J. Cell Sci.* 109:3089–3102.

Pazour, G.J., B.L. Dickert, Y. Vucica, E.S. Seeley, J.L. Rosenbaum, G.B. Witman, and D.G. Cole. 2000. *Chlamydomonas IFT88* and its mouse homologue, polycystic kidney disease gene *tg737*, are required for assembly of cilia and flagella. *J. Cell Biol.* 151:709–718. http://dx.doi.org/10.1083/jcb.151.3.709

Pugacheva, E.N., and E.A. Golemis. 2005. The focal adhesion scaffolding protein HEF1 regulates activation of the Aurora-A and Nek2 kinases at the centrosome. *Nat. Cell Biol.* 7:937–946. http://dx.doi.org/10.1038/ncb1309

Pugacheva, E.N., S.A. Jablonski, T.R. Hartman, E.P. Henske, and E.A. Golemis. 2007. HEF1-dependent Aurora A activation induces disassembly of the primary cilium. *Cell*. 129:1351–1363. http://dx.doi.org/10.1016/j.cell.2007.04.035

Quarmby, L.M., and J.D. Parker. 2005. Cilia and the cell cycle? *J. Cell Biol.* 169:707–710. http://dx.doi.org/10.1083/jcb.200503053

Rieder, C.L., C.G. Jensen, and L.C. Jensen. 1979. The resorption of primary cilia during mitosis in a vertebrate (PtK1) cell line. *J. Ultrastruct. Res.* 68:173–185. http://dx.doi.org/10.1016/S0022-5320(79)90152-7

Robert, A., G. Margall-Ducos, J.E. Guidotti, O. Brégerie, C. Celati, C. Bréchot, and C. Desdouets. 2007. The intraflagellar transport component IFT88/polaris is a centrosomal protein regulating G1-S transition in non-ciliated cells. *J. Cell Sci.* 120:628–637. http://dx.doi.org/10.1242/jcs.03366

Roghi, C., R. Giet, R. Uzbekov, N. Morin, I. Chartrain, R. Le Guellec, A. Couturier, M. Dorée, M. Philippe, and C. Prigent. 1998. The *Xenopus* protein kinase pEg2 associates with the centrosome in a cell cycle-dependent manner, binds to the spindle microtubules and is involved in bipolar mitotic spindle assembly. *J. Cell Sci.* 111:557–572.

Satir, P., and S.T. Christensen. 2007. Overview of structure and function of mammalian cilia. *Annu. Rev. Physiol.* 69:377–400. http://dx.doi.org/10.1146/annurev.physiol.69.040705.141236

Schmidt, T.I., J. Kleylein-Sohn, J. Westendorf, M. Le Clech, S.B. Lavoie, Y.D. Stierhof, and E.A. Nigg. 2009. Control of centriole length by CPAP and CP110. *Curr. Biol.* 19:1005–1011. http://dx.doi.org/10.1016/j.cub.2009.05.016

Singla, V., and J.F. Reiter. 2006. The primary cilium as the cell's antenna: signaling at a sensory organelle. *Science*. 313:629–633. http://dx.doi.org/10.1126/science.1124534

Sugimoto, M., A. Inoko, T. Shiromizu, M. Nakayama, P. Zou, S. Yonemura, Y. Hayashi, I. Izawa, M. Sasoh, Y. Uji, et al. 2008. The keratin-binding protein Albatross regulates polarization of epithelial cells. *J. Cell Biol.* 183:19–28. http://dx.doi.org/10.1083/jcb.200803133

Tang, C.J., R.H. Fu, K.S. Wu, W.B. Hsu, and T.K. Tang. 2009. CPAP is a cell-cycle regulated protein that controls centriole length. *Nat. Cell Biol.* 11:825–831. http://dx.doi.org/10.1038/ncb1889

Tucker, R.W., A.B. Pardee, and K. Fujiwara. 1979. Centriole ciliation is related to quiescence and DNA synthesis in 3T3 cells. *Cell*. 17:527–535. http://dx.doi.org/10.1016/0092-8674(79)90261-7

Vecchione, A., M. Fassan, V. Anesti, A. Morrione, S. Goldoni, G. Baldassarre, D. Byrne, D. D'Arca, J.P. Palazzo, J. Lloyd, et al. 2009. MITOSTATIN, a putative tumor suppressor on chromosome 12q24.1, is downregulated in human bladder and breast cancer. *Oncogene*. 28:257–269. http://dx.doi.org/10.1038/onc.2008.381

Walter, A.O., W. Seghezzi, W. Korver, J. Sheung, and E. Lees. 2000. The mitotic serine/threonine kinase Aurora2/AIK is regulated by phosphorylation and degradation. *Oncogene*. 19:4906–4916. http://dx.doi.org/10.1038/sj.onc.1203847

Wang, X.X., R. Liu, S.Q. Jin, F.Y. Fan, and Q.M. Zhan. 2006. Overexpression of Aurora-A kinase promotes tumor cell proliferation and inhibits apoptosis in esophageal squamous cell carcinoma cell line. *Cell Res.* 16:356–366. http://dx.doi.org/10.1038/sj.cr.7310046

Wheatley, D.N., A.M. Wang, and G.E. Strugnell. 1996. Expression of primary cilia in mammalian cells. *Cell Biol. Int.* 20:73–81. http://dx.doi.org/10.1006/cbir.1996.0011